A comparative study on ganglioside micelles using electronic energy transfer, fluorescence correlation spectroscopy and light scattering techniques

Radek Šachl,[ab] Ilya Mikhalyov,†[a] Martin Hof[b] and Lennart B. Å. Johansson*[a]

Received 3rd December 2008, Accepted 18th February 2009
First published as an Advance Article on the web 25th March 2009
DOI: 10.1039/b821658d

Ganglioside (G_{M1}) micelles have been studied by means of three different techniques: fluorescence correlation spectroscopy (FCS), electronic energy transfer, as monitored by time-resolved fluorescence spectroscopy, as well as static and dynamic light scattering. The aggregation numbers obtained, 168 ± 4, remain constant over a wide range of G_{M1} concentrations (0.764–156 μM), are very consistent when using different donor–acceptor energy transfer pairs and have served as reference values in tests of the FCS method. It is recommended to calibrate the focal volume by using known dye concentrations. For this the rhodamine dye, 5-TAMRA, turns out to be most suitable. It is also shown that FCS provides correct values of the aggregation numbers, provided that the focal volume is calibrated by using updated values of the diffusion constant of Rhodamine 6G. These results also support recent methodological advances in FCS.

Introduction

G_{M1} gangliosides are amphiphilic molecules whose hydrophobic part consists of a sphingosine and a fatty acid, while the bulky hydrophilic part is built up by several sugar units. One of these is a negatively charged sialic acid. In all vertebrate cells, the gangliosides are generally expressed in the outer leaflet of the plasma membrane but are also found in endocytic organelles, trans-Golgi network and in nuclear membranes.[1,2] The gangliosides are thought to be involved in various biological processes, such as cell–cell recognition and interaction, as well as signal transduction.[3,4] G_{M1} is also present in detergent resistant domains (rafts)[5–7] and exhibits self-aggregation in model lipid membranes.[8]

Frequently, the G_{M1} ganglioside is discussed in the context of Alzheimer′s disease, which is associated with the formation of amyloid deposits in the human brain. The deposits mainly consist of aggregates of amyloid β-peptides accompanied by G_{M1}.[1,9] On the other hand, the disease G_{M1} *gangliosidosis* is caused by a deficiency of the β-galactisidase enzyme, which causes lysosomal swelling, cell damage and organ dysfunction.[10] It has also been speculated whether G_{M1} molecules serve as receptors for the cholera toxin.[11,12]

Due to its bulky headgroup, the G_{M1} lipid forms micelles over a broad range of concentrations ($\geq 2.10^{-8}$ M) in water, which also includes physiological conditions.[3,13–15] The reported aggregation numbers (N) of G_{M1} micelles suggest strong temperature dependence. Upon heating, the value of N remains constant up to 30 °C and then it decreases almost linearly from 30 to 55 °C. Then, upon lowering the temperature, the N-value is not changed. The co-existence of two molecular conformations of the G_{M1} chains has been suggested to be a possible explanation for this.[16,17] According to the model, heating promotes the transition from states of higher N-values to lower ones. Upon cooling, the reverse transition is not observed due to the long equilibration time needed. However, this explanation is not supported by the data of Orthaber and Glatter[18] who, in addition to small G_{M1} micelles, also observed larger aggregates. It was therefore concluded that the decrease of the aggregation numbers is caused by the poor solubility of G_{M1} in water.

In the present study, the aggregation numbers of G_{M1} micelles have been determined by using fluorescence correlation spectroscopy (FCS) and electronic energy transfer (ET) experiments, as well as static/dynamic light scattering (LS). LS provides information about the polydispersity of the system and was applied here to reinvestigate the controversial temperature behaviour of G_{M1} micelles. In addition, it yielded mass average aggregation numbers, N^{LS}, and hydrodynamic radii, R_H^{LS}, of G_{M1} micelles. Both quantities have been studied by two other techniques. In order to determine the aggregation numbers from FCS experiments, a precise knowledge of the focal volume is needed. Although FCS experiments can provide an absolute value of the diffusion constant or the concentration[19–21] (and consequently N^{FCS}), the applicability is mostly restricted to measuring relative values. This can be ascribed to the experimental difficulty in obtaining an accurate determination of the focal volume (V_f).[22] Actually, the value obtained for V_f is, in fact, influenced by external factors such as variation of the sample refractive index, optical saturation and optical alignment.

To accurately determine the focal volume, two different procedures have been applied. The calibration methods, which

[a] *Department of Chemistry, Biophysical Chemistry, Umeå University, S-901 87, Umeå, Sweden. E-mail: lennart.johansson@chem.umu.se*
[b] *J. Heyrovský Institute of Physical Chemistry of the Academy of Sciences of the Czech Republic, Dolejškova 3 182 23 Prague 8, Czech Republic*
† Permanent address: Shemyakin & Ovchinnikov Institute, Institute of Bioorganic Chemistry, Russian Academy of Sciences, Moscow, Russia

make use of known dye concentrations, involve no approximations concerning the shape of V_f but they are elaborate and time consuming. On the other hand, the calibration method which assumes a known diffusion constant is very fast but comprises assumptions regarding the shape of V_f, as well as the precise value of the diffusion constant. In the past, the latter method has been proved to be technically difficult. However, two recent publications[23,24] report values on the translational diffusion constant of Rhodamine 6G (R6G), which is a compound frequently used for calibrating V_f. Both values obtained differ substantially from the value[25] that has hitherto been used for more than three decades. To probe the different calibration methods of FCS by making use of the updated diffusion constant of R6G, electronic energy transfer experiments were applied, which provided independent values of aggregation numbers. In the ET experiments, three DA pairs have been used. Some of the ET and FCS experiments were performed in the range of physiological G_{M1} concentrations.

Materials and methods

Chemicals

Tetra-2,5,8,11-*tert*-butylperylene was synthesised as reported previously,[26] perylene was purchased from Sigma Aldrich. BODIPY-FL-G_{M1} was synthesized as described elsewhere.[8] 564/570-BODIPY-G_{M1} was synthesized as described elsewhere[27] and the G_{M1} ganglioside was isolated from bovine brain as described by Svennerholm.[28] Octadecylrhodamine B (ORB), 5-TAMRA and Rhodamine 6G were purchased from Molecular Probes and tris(hydroxymethyl)aminomethane hydrochloride from Sigma Aldrich.

Preparation of G_{M1} micelles

Appropriate amounts of G_{M1}, with respect to the experimental technique, were dissolved in a chloroform–methanol mixture (2 : 1, v/v) to which the desired amount of fluorophore was added. ORB was an exception because it was dissolved in ethanol and then immediately added into the aqueous lipid solution. The concentration of ethanol was kept below 1% by volume. After the evaporation of the organic solvents, the sample was dried under high vacuum for 3 h. The obtained lipid film was hydrated to the desired concentration by adding a TRIS-HCl buffer (pH 7.4) containing 150 mM NaCl.

Light scattering (LS)

The light scattering equipment (ALV, Langen, Germany), which enables static and quasi-elastic light scattering measurements, consists of a 633 nm He–Ne laser, a goniometer (ALV CGS/8F), a detector (ALV High QE APD) and a multi-bit multi-tau autocorrelator (ALV 5000/EPP). The measurements were carried out on lipid solutions with differing mass concentrations (4–10 g L^{-1}) at different angles ranging from 30 to 150° at 21 °C. All lipid samples were filtered through 0.45 μm Acrodisc filters after ensuring that the solution did not contain G_{M1} particles larger than the pore dimensions.

The obtained static LS intensities were used to construct Zimm plots according to:

$$\frac{Kw}{\Delta R(\theta, w)} = \frac{1}{P(\theta)M_w} + 2A_2 w. \quad (1)$$

The constant $K = 4\pi^2 n_0^2 (dn/dc)^2/\lambda^4 N_A$ depends on the refractive index of the solvent (n_0) and the refractive index increment of the scattering object in the solution (dn/dc), the wavelength of incident light (λ) and Avogadro's number (N_A). The excess Rayleigh ratio [$\Delta R(\theta, w)$] is measured at an angle (θ) between the incident and scattered light and depends on the lipid mass concentration (w). $P(\theta)$ stands for the particle scattering function, which describes the angular dependence of the scattered intensity, M_w is the mass-average molar mass of the particles and A_2 is the "light-scattering-averaged" osmotic second virial coefficient of the solution. Further details are given elsewhere.[29]

The refractive index increment of G_{M1} in water was measured by means of a Brice–Phoenix differential refractometer. The obtained value $dn/dc = 0.147$ cm^3 g^{-1} is in perfect agreement with previously published data.[16]

The evaluation of the dynamic light scattering data is based on the analysis of the measured normalized autocorrelation function, $g_2(t)$, which is related to the electric field autocorrelation function, $g_1(t)$ by the Siegert relation; $g_2(t) = g_1(t) + \beta|g_1(t)|^2$. The distribution of relaxation times $\tau A(\tau)$ can be expressed as the inverse Laplace transform according to

$$g_1(t) = \int_0^\infty \tau A(\tau) \exp(-t/\tau) d\ln \tau. \quad (2)$$

This is conveniently performed by using the constrained regularisation algorithm (CONTIN).

To obtain the averaged hydrodynamic radius of the particles, R_H (z-average for R_H^{-1}), the $g_1(t)$ functions for various G_{M1} concentrations and scattering angles were fitted to the second order cumulant expansion:

$$g_1(t) = \exp(-D_{app} q^2 t + \mu_2 t^2/2), \quad (3)$$

where D_{app} is the apparent translational diffusion constant and μ_2 (the 2nd cumulant) is the second moment of the distribution function of relaxation times and $q = 4\pi n_0 \sin(\theta/2/\lambda)$ is the magnitude of the scattering vector $\boldsymbol{q}$. The obtained D_{app} values were further extrapolated to zero q and c to yield the z-averaged diffusion constant of the particles, $\langle D \rangle_z$, using the relationship[29]

$$D_{app}(q,c) = \langle D \rangle_z (1 + k_D c + C R_g^2 q^2). \quad (4)$$

In eqn (4) k_D is the hydrodynamic virial coefficient and C is a coefficient determined by the slowest internal motion and polydispersity of the scattering particles. R_g denotes the radius of gyration. The hydrodynamic radius was calculated from $\langle D \rangle_z$ and the Stokes–Einstein equation, $R_H = k_B T/6\pi \eta_0 \langle D \rangle_z$ in which η_0 is the viscosity of the solvent and k_B and T have their usual meaning.

Aggregation numbers determined by using light scattering (LS)

LS experiments yield information concerning the micellar aggregation number (N^{LS}) from the mass-averaged molar mass (M_w) derived from a Zimm graph, according to the following relation;

$$N^{LS} = \frac{M_w}{M}. \quad (5)$$

Here, M is the molecular mass of the monomer molecule, *i.e.* G_{M1}.

Time-correlated single-photon counting

Fluorescence lifetime decays were measured with an instrument from IBH Consultants Ltd (Glasgow, Scotland) equipped with dichroic sheet polarisers. The pulsed excitation source was a laser diode with intensity maximum centred either at 404 or 467 nm. The laser repetition rate was approximately 800 kHz and the count rate never exceeded 1% of this rate. The excitation and emission wavelengths were selected by monochromators. The fluorescence lifetime decays were measured with the emission polariser set at the magic angle (54.7°) relative to the excitation polariser. The instrumental response function, $I(t)$, was determined by using a light scattering solution (LUDOX). The true fluorescence decay $f(t)$, was approximated by a sum of exponential functions, and obtained by using a deconvolution method based on the Levenberg–Marquard algorithm,[30,31] which accounts for the following equations;

$$F(t) = \int_0^t I(t-t')f(t')\mathrm{d}t' \quad (6)$$

$$f(t) = \sum_{i=1}^{m} a_i \exp(-t/\tau_i) \qquad \sum_{i=1}^{m} a_i = 1 \quad (7)$$

where $F(t)$ stands for the measured fluorescence decay and τ_i is the lifetime of the ith component. The fluorescence decays recorded for the reference sample as well as the samples containing donors and acceptors have been fitted over the same time span.

Aggregation numbers determined by using energy transfer (ET)

The idea of using electronic energy transfer for determining micellar aggregation numbers (N^{ET}) rests on fluorescence quenching methods which have previously been developed.[32–34] For ET studies, two different samples are needed. One serves as a reference system and contains donor molecules solubilised in the micelles, while donors as well as acceptors (A) are solubilised in the second sample. In the analysis of fluorescence data it is assumed that all acceptors are distributed among micelles according to Poisson statistics. Hence the probability of finding n acceptors in a micelle is given by $P_n = \langle n\rangle^n \exp(-\langle n\rangle)/n!$, where $\langle n\rangle$ denotes the average number of acceptors per micelle.

To calculate N^{ET}, it is necessary to determine $\langle n\rangle$ from experiments. Having knowledge of the acceptor concentration ([A]), the total lipid concentration and the critical micelle concentration (cmc), the aggregation number can be calculated according to the relation: $N^{ET} = ([\text{Lipid}]-\text{cmc})\langle n\rangle/[\text{A}]$. Provided the rate of migration of donors and acceptors among the micelles is negligible, the fraction of micelles lacking acceptor molecules is given by $\langle n\rangle = -\ln P_0$, which is related to the experimental fluorescence intensities in the presence ($F_A(t)$) and absence ($F_0(t)$)) of acceptors. This equation reads:

$$\langle n\rangle = -\ln P_0 = -\ln \frac{F_A(t > t_{lim})}{F_0(t > t_{lim})}. \quad (8)$$

To obtain the correct value of $\langle n\rangle$, the fluorescence intensities in eqn (8) that must be used are at times ($t \geq t_{lim}$) for which all micelles containing donors accessible to acceptors have been quenched (*cf.* Fig. 4).

Fluorescence correlation spectroscopy (FCS)

FCS measurements were performed using an upgraded Confocor 19 (Carl Zeiss GmbH, Jena; Evotec Biosystems GmbH, Hamburg; PicoQuant GmbH, Berlin, Germany).[35] Briefly, it consists of an inverted confocal microscope Axiovert 100 with a water immersion objective C-Apochromat40_/1.2 W, an adjustable pinhole, cw He/Ne 543 nm laser, original Zeiss' filters, a single-photon counting detector SPCM-AQR-13-FC (Perkin-Elmer, Fremont, MA), and a time-tagged time-resolved (TTTR) data-storing card TimeHarp 200 (PicoQuant GmbH, Berlin, Germany). FCS data fitting was performed with the OriginPro70 software package (OriginLab Corp., Northampton, MA) using home-written macros. The laser intensity ranged from 1.37 to 13.7 μW, depending on the dye concentration. Within each experimental set, the intensity remained unaltered. The principles of FCS are further outlined elsewhere.[36]

For a free 3D translational diffusion, the fluorescence intensity correlation function is related to the fraction of fluorescent molecules converted to the triplet state (ϕ_T) and the triplet state lifetime (τ_T) according to[37]

$$G(t) = 1 + \frac{1}{1 + \frac{t}{\tau_D}\sqrt{1 + \frac{t}{P_s^2\tau_D}}} \frac{G^T(\phi_T, \tau_T)}{N_p}. \quad (9)$$

In eqn (9) N_p is the particle number expressing the number of fluorophores in the illuminated focal volume, $P_s = b/a$ is the structure parameter, where b and a are the long and short axes of the 3D gaussian focal volume (V_f). The diffusion correlation time (τ_D) is related to the diffusion constant $D = a^2/4\tau_D$ and, finally, $G^T(\phi_T,\tau_T)$ is a function which accounts for the intersystem crossing to the triplet state:

$$G^T(\phi_T, \tau_T) = \frac{1 - \phi_T + \phi_T \exp(-t/\tau_T)}{1 - \phi_T}. \quad (10)$$

Aggregation numbers determined by using fluorescence correlation spectroscopy (FCS)

Provided all micelles contain at least one fluorescent label visible for FCS, the aggregation numbers are obtained from

$$N^{FCS} = \frac{[\text{Lipid}] - \text{cmc}}{[\text{Mic}]^{FCS}} \quad (11)$$

If the number of particles (N_p) obtained from the fluorescence correlation $G(t)$ equals the number of micelles found in the focal volume, the concentration of micelles is given by

$$[\mathrm{Mic}]^{\mathrm{FCS}} = \frac{N_{\mathrm{p,lim}}}{N_A V_f}, \qquad (12)$$

where $N_{\mathrm{p,lim}}$ is the limiting particle number and V_f is the focal volume.

Results and discussion

One main goal of the present study concerns the comparison of the aggregation number of G_{M1} micelles as obtained by means of three physically different experimental approaches. Prior to this comparison, it is necessary to characterise the micelles with respect to temperature since there is a controversy among previous investigations.[17,18] Static and dynamic light scattering (LS) experiments have been used for this purpose.

Characterisation of G_{M1} micelles by LS techniques

The LS from freshly prepared G_{M1} micelles in a TRIS-HCl buffer was studied at a scattering angle of 90°. The Laplace transform of dynamic LS correlation curves provides a distribution of relaxation times, which contains information about the polydispersity of the system. The distribution reveals one narrow peak, centred at *ca.* 0.07 ms (*cf.* Fig. 1), which corresponds to a hydrodynamic radius $R_H \approx 5.4$ nm. A more precise value of the apparent diffusion coefficient was obtained by an extrapolation to the zero concentration and the zero scattering angle. The value thus obtained, 5.9 ± 0.03 nm, agrees very well with the value published by Brocca *et al.* (5.87 nm),[38] as well as that found by Orthaber and Glatter (5.75 nm).[18] In the latter study, this value was observed after larger aggregates were completely dissolved over time (*vide infra*). To ensure that no larger particles were lost in the filtering procedure, the samples in this study were examined before and after filtration. No significant difference was observed.

Except for the aggregate size reported above, no G_{M1} aggregates were detected in the range between 0.1 and

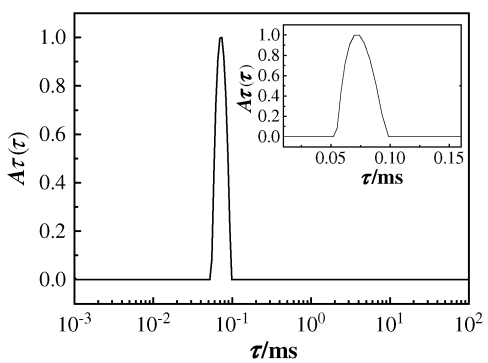

Fig. 1 Dynamic light scattering relaxation time distributions (measured at the scattering angle 90° and at the temperature 21 °C) of G_{M1} micelles. The lipid concentration in the TRIS buffer was 10 g L^{-1}. **Insert:** zoomed region of the peak in Fig. 1.

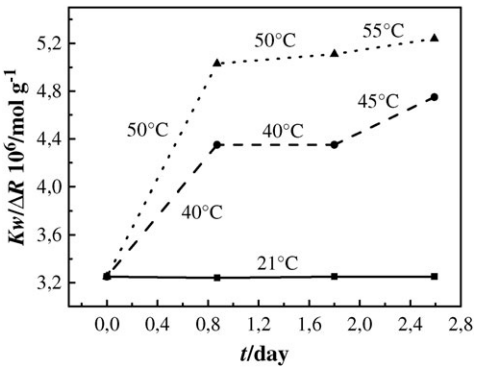

Fig. 2 $Kw/\Delta R$ proportional to $1/M_w^{app}$, where M_w^{app} is the apparent molar mass of G_{M1} micelles at different heating cycles (see the text). Solid line: reference sample with no heating, dashed line: heating up to 40 °C until the sample is equilibrated and then up to 45 °C, dotted line: heating up to 50 °C until the sample is equilibrated and then up to 55 °C. The concentration of the lipid was 7 g L^{-1}.

5000 nm. Furthermore, the distribution did not change within several days. These results contradict the study by Orthaber and Glatter,[18] who observed one main peak at *ca.* 4.5 nm and two more peaks at *ca.* 100 and 1000 nm. The latter peaks disappeared, however, within 42 days at room temperature. This has been interpreted as a slow dissolution of higher aggregates due to the poor solubility of G_{M1} in water. On the other hand, neither Brocca *et al.*[17] nor Cantù *et al.*[16] report on the presence of larger aggregates. If the aggregation number changes then it would be induced by a shift in temperature and would not be a consequence of poor G_{M1} solubility. In this work, repeating studies of the temperature behaviour of G_{M1} micelles gave similar results to those obtained by Cantù *et al.* Three identical samples were exposed to three different heating cycles (*cf.* Fig. 2), where one sample served as a reference and was kept at 21 °C during the whole experiment. The second sample was heated to 40 °C during approximately one day, cooled to, and measured at, 21 °C. It was then heated again to 40 °C in order to check whether the sample had already reached its equilibrium and finally heated up to 45 °C and measured again at room temperature. The third sample was exposed to the identical cycle as the second one at 50 and 55 °C. The results are summarized in Fig. 2, where $Kw/\Delta R$ is plotted as a function of time. Note that $Kw/\Delta R$ is inversely proportional to the apparent molecular mass. This confirms that, for one population of micelles, the aggregation numbers do irreversibly decrease upon heating but are not further changed upon repeated cooling. Thus, the decrease in the average aggregation number is not the result of a slow dissolution of larger aggregates.[18] Cantù *et al.*[16,17] have proposed a "cooperative transition model", which assumes the co-existence of two molecular conformations of the G_{M1} molecules in micelles. Upon heating, an energetically more favourable conformation is adopted, whereas cooling leads to a metastable state due to a long equilibration time. Experiments carried out by Brocca *et al.*[17] support this model.

Taken together, it is concluded that the G_{M1} micelles exhibit a relatively narrow size distribution. Moreover, the SAXS experiments show that the aggregation numbers of G_{M1} are concentration independent in the range of *ca.* 0.1 to 100 mM.[38]

Aggregation numbers obtained from LS experiments

The Zimm plot for G_{M1} micelles was obtained by measuring the scattered light intensity at different angles and concentrations (Fig. 3). Since the micelles are small, the scattering particle function $P(\theta) \approx 1$ for all scattering angles. Therefore, Kw/R exhibits only a weak linear dependence. An extrapolation to zero concentration and zero scattering angle yields the micellar molar mass $M_w = (4.07 \pm 0.07) \times 10^5$ g mol^{-1}, from which the aggregation number, $N^{LS} = 263 \pm 5$, and the molar mass of G_{M1}, $M(G_{M1}) = 1546$ g mol^{-1}, were calculated using eqn (5) . Cantù *et al.*[16] obtained a slightly higher value of $N^{LS} \approx 300$, most likely since their value of $Kw/\Delta R$ was not extrapolated to the zero concentration.

One should realize that when evaluating LS data, the N^{LS} values are usually calculated by dividing the mass-average molar mass of a micelle with the number-average molar mass of a monomer. Instead, the value of M_w should be used, provided the degree of polydispersity is not negligible. This is not an important issue since, in the present study, the G_{M1} monomers form a uniform distribution. It is also important to carefully determine the refractive index increment (dn/dc) because $1/M_w$ depends on its square (*cf.* Materials and methods).

Aggregation numbers obtained from ET

LS experiments yield a weight-average molar mass from which N^{LS} can be calculated, whereas the ET and FCS techniques provide the number-averaged aggregation number (N^X, X = ET or FCS). For a perfectly monodisperse distribution these aggregation numbers would all be the same. In the following, donor–acceptor energy transfer experiments are applied and the fact that $N^{ET} = N^{FCS}$ within experimental errors, which can be used to calibrate and evaluate different approaches to the analysis of FCS data. Three different DA pairs, solubilised in G_{M1} micelles with different Förster radii, were used in separate studies. In one system studied, BODIPY-FL-G_{M1} transfers its excited electronic energy to 564/571-BODIPY- G_{M1}, which hence serves as the acceptor (R_0 = 58.7 Å). Both BODIPY groups were covalently linked in the non-polar part of G_{M1}. The fluorescence relaxation of the donor in the absence of the acceptor shows a major lifetime component of 6.1 ns (96%) and a minor one of 2.4 ns. Similar results have been observed in other studies.[39] In the presence of acceptors,

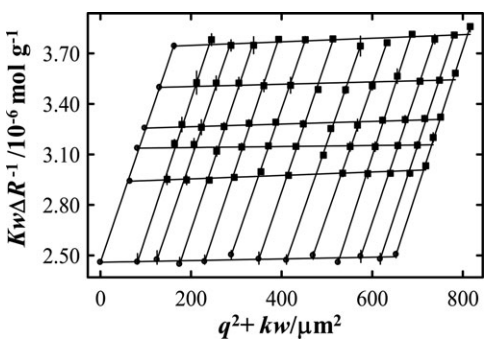

Fig. 3 The Zimm plot obtained for G_{M1} micelles at 21 °C. The lipid concentrations ranged from 10 to 4 g L^{-1} and the scattering angle from 40 to 150°.

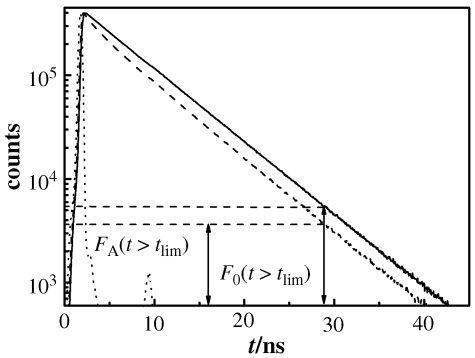

Fig. 4 The instrumental response function (dotted curve) together with the fluorescence decay curves of the donor BODIPY-FL-G_{M1}, in the absence (solid curve) and presence (dashed curve) of the acceptor 564/571-BODIPY-G_{M1}, when solubilised in G_{M1} micelles. F_0 ($t \geq t_{lim}$) and F_A ($t \geq t_{lim}$) denote fluorescence intensities in absence and presence of the acceptor (*cf.* eqn (8)). The G_{M1} concentration was 158×10^{-4} μM and the concentrations of the donor and the acceptor were 0.657 and 0.483 μM, respectively.

the decay of the donor is much more complex but it can be nicely fitted to a sum of three exponential functions. The addition of a fourth component did not improve the quality of the fit and the value of N^{ET} remained unaltered. The fluorescence decays for this DA pair are depicted in Fig. 4, and the corresponding aggregation numbers are summarised in Table 1.

Perylene and BODIPY-FL-G_{M1} were used as a second DA pair (R_0 = 49.6 Å). The reference system, *i.e.* perylene in G_{M1} micelles, exhibits a multi-exponential fluorescence relaxation, which is likely to be due to the formation of dimers. The physical details of the fluorescence relaxation are, however, not needed in the analysis of the DA system by using eqn (8). This is because the measured decays of the DA system were always compared with the obtained decays for the reference system, which contains only donors. Indeed, the obtained aggregation numbers are very similar to those found for the above system (*cf.* Table 1). The invariance with respect to a complex photophysics decay of the donor is further supported by experiments where perylene was replaced by TBPe and BODIPY-FL-G_{M1} was the acceptor (R_0 = 50.7 Å). Here, the donor fluorescence is almost a single exponential function, which can be ascribed to the bulky *tert*-butyl groups having the ability to suppress the formation of dimers. The analysis of this DA system yields very similar aggregation numbers to those found for the previously described DA pairs (*cf.* Table 1).

Table 1 Aggregation numbers (N^{ET}) determined from the time-resolved fluorescence relaxation experiments using different donor and acceptor pairs at 21 °C. The average aggregation number obtained from these experiments is $\bar{N}^{ET} = 168 \pm 4$

Donor	Acceptor	$[G_{M1}]$/M	N^{ET}
BODIPY-FL-G_{M1}	564/571-BODIPY-G_{M1}	$1.56\ 10^{-4}$	172
BODIPY-FL-G_{M1}	564/571-BODIPY-G_{M1}	$1.59\ 10^{-4}$	166
BODIPY-FL-G_{M1}	564/571-BODIPY-G_{M1}	$1.59\ 10^{-5}$	166
TBPe	BODIPY-FL-G_{M1}	$1.56\ 10^{-4}$	172
Perylene	BODIPY-FL-G_{M1}	$1.46\ 10^{-4}$	164

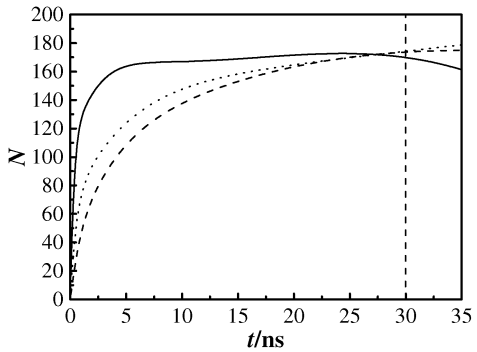

Fig. 5 G_{M1} aggregation numbers obtained using ET (N^{ET}) are plotted as a function of time elapsed after the excitation for three different DA pairs: BODIPY-FL-G_{M1} & 564/571-BODIPY-G_{M1} (dotted line, $[G_{M1}] = 158$ μM); perylene & BODIPY-FL-G_{M1} (dashed line, $[G_{M1}] = 147$ μM); TBPe & BODIPY-FL-G_{M1} (solid line, $[G_{M1}] = 158$ μM).

An important requirement of the ET technique is the energy transfer rate, which must be fast enough to ensure the detection of donor fluorescence originating also from solely acceptor-free micelles. In other words, the reference decay curve and the quenched fluorescence decay must become mutually parallel within the time window of a measurement. This requirement could be difficult to fulfil for larger particles, whose size exceeds the Förster radius considerably ($k \sim 1/R^6$). As illustrated in Fig. 5, the apparent aggregation number reaches a constant limiting value (the 'true' N) at approximately 10 ns after an excitation pulse in the case of TBPe and BODIPY-FL-G_{M1}, and after *ca.* 30 ns for the two DA pairs studied.

The approach used here for determining N^{ET}, differs somewhat from that developed by Tachiya *et al.*[34] In particular, the data cannot be fitted to a theoretical model that assumes *one* rate constant of quenching. This could also be expected if one recalls that the electronic transfer rate strongly depends on the DA distance and the spatial distribution of donor and acceptor groups present in the micelles. Despite this deviation from the Tachia model, the method presented here works very well, also when the quenching mechanism is Förster energy transfer.

Aggregation numbers obtained from FCS

Fluorescence correlation spectroscopy (FCS) provides a useful technique for investigating nanoparticles and their aggregation properties. In the present study of aggregation numbers, the FCS experiment concerns determining the number of fluorophore labelled micelles within a focal volume. For this, the choice of suitable fluorescent molecules is crucial. For the following reasons, octadecylrhodamine B (ORB) was used: (i) the long hydrophobic chain of ORB leads to relatively high affinities to detergents;[19] (ii) the fluorescence intensity from the small fraction, which theoretically might be dissolved in the bulk phase, is effectively self-quenched and, consequently, it has a negligible contribution to intensity fluctuations; (iii) the rate of intersystem crossing is low; (iv) the self-quenching of ORB in nanoparticles allows an increase of the ORB : G_{M1} molar ratio without considerable changes of fluorescence intensity.[19]

For the calculation of the aggregation numbers from FCS data the total concentration of G_{M1} ($[G_{M1}]$), the concentration of micelles in the bulk, as well as the critical micelle concentration, are needed (*cf.* eqn (11), (12)). Here $[G_{M1}]$ is *a priori* known, as well the value of cmc(G_{M1}) = 200 μM.[40,41] The concentration of micelles ($[Mic]^{FCS}$) has been calculated by using the parameters obtained from the FCS experiments (eqn (12)). Since emission is only observed from micelles containing one or several fluorophores, every micelle needs to be labelled in the FCS experiments. This certifies that the correct number of micelles in the focal volume divided by the size of the focal volume and Avogadro constant (eqn (12)) is equal to the concentration of micelles in the sample. Therefore the ORB : G_{M1} ratio is increased stepwise until a limiting plateau of the particle number (N_p) is reached, as is shown in Fig. 6(a). This ensures that every micelle is visible in the FCS experiment. Note that quenching influences the ORB : G_{M1} ratio at which the limiting plateau starts. It might therefore be that only micelles containing two or more ORB molecules are detected. In order to visualise a micelle, it is possible to estimate the average number of probes/micelles needed by assuming a Poisson distribution of the ORB molecules among the micelles.[19] In the case of G_{M1}, one needs a ratio of $[ORB]/[G_{M1}] = 0.04$, which corresponds to a probe to micelle ratio of about six (*cf.* Fig. 6(a)). The number of particles needed to calculate $[Mic]^{FCS}$ was obtained by fitting the fluorescence intensity correlation curves $G(t)$ to the model described above (*cf.* eqn (9), (10)). All correlation curves (*cf.* Fig. 6(b)) can be nicely fitted to a uniform size distribution of G_{M1} micelles. There is then no reason to involve a second diffusion coefficient in the model, ascribed to freely moving ORB molecules/aggregates in the bulk phase. Moreover, the addition of ORB to an excess of GM1 micelles ($[ORB]/[GM1] = 4.4 \times 10^{-5}$, [GM1] = 0.32 mM) results in a 67-fold increase in the intensity as compared to the intensity of the same amount of ORB molecules dissolved in the buffer. Similarly, for the GM1 concentrations used in the FCS experiments ($[G_{M1}] = 15.4$ μM and $[G_{M1}] = 0.744$ μM) and the ratio $[ORB]/[GM1] = 1.7\ 10^{-2}$, the intensity increases 44–49 times upon binding. The intensity does not change much (from 49 to 67) for a 430 fold increase of the GM1 concentration at a constant ORB concentration. However, it changes considerably when compared to the pure buffer. It is therefore concluded that only the ORB molecules that are solubilised into G_{M1} micelles are monitored. The partition coefficient for the PS–PMA micelles has been estimated to be *ca.* 10^5. In the optimisation of the five free parameters in eqn (9) it was observed that the obtained values of N_p were not particularly sensitive to a restriction of the number of parameters used.

The accuracy of focal volume estimation (V_f) is crucial for the determination of diffusion constants and micelle aggregation numbers.[22] For instance, the focal volume is influenced by changes of the refractive index, as well as saturation effects. This implies that the calibration and the experiments must be performed under the same conditions. For the different rhodamine derivatives studied here, the intensities used were adapted to avoid any saturation.

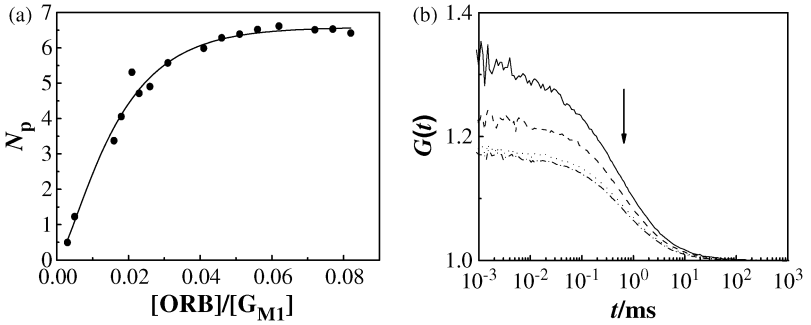

Fig. 6 (a): Dependence of the particle number (N_p) as a function of the molar probe : G_{M1} ratio. (b): Fluorescence intensity correlation curves $G(t)$ for increasing probe : G_{M1} ratios. [G_{M1}] = 0.764 μM, [ORB] = 7.74 nM (dash-dot line), 23 nM (dotted line), 42 nM (dashed line) and 45.8 nM (solid line). The arrow indicates the increase in particle number with increasing probe : G_{M1} ratio.

In the calibration of V_f, the rhodamine derivative, 5-TAMRA, of known bulk concentration was used. Measurement of the number of particles in V_f as a function of [5-TAMRA] gives a linear dependence which is described by the equation: $N_p = N_A V_f$[5-TAMRA]. Thus, V_f can be calculated from the slope (*cf.* Fig. 7). Frequently used dyes in FCS, *e.g.* R6G and Rhodamine B, are not suitable for the calibration due to their adsorption onto the cuvette surfaces. From the present work however, 5-TAMRA turns out to be very suitable for the calibration of the focal volume.

The known value of the translational diffusion constant for R6G has been used as a second calibration method for V_f. Assuming that the focal volume may be approximated by $V_f = \pi^{3/2} a^2 b$ it is possible to calculate V_f from the relation:

$$V_f = (4\pi\tau_D D_{R6G})^{3/2} P_s. \quad (13)$$

In eqn (13), D_{R6G} denotes the translational diffusion constant of R6G. This calibration method is much faster than the one described above, but less accurate due to the uncertainty in P_s.

The determination of V_f also depends on the accuracy of the diffusion constant. It is experimentally difficult to measure the diffusion constant at infinite dilution. More than thirty years ago Madge *et al.*[25] published a value of D_{R6G}(Ma) = 280 μm^2 s^{-1} for R6G dissolved in water at 22 °C. Since then this value has been used in numerous publications. Recently, the development of FCS has made it possible to more accurately determine the diffusion constant. Petrášek and Schwille[24] have used scanning FCS and obtained D_{R6G}(P) = 426 μm^2 s^{-1} in water at 22.5 °C, while Müller *et al.*[23] have applied multi-colour dual-focus FCS and obtained D_{R6G}(Mü) = 414 μm^2 s^{-1} in water at 25 °C. A recalculation of the D values to 22.5 °C yields D_{R6G}(Ma) = 284 μm^2 s^{-1}, D_{R6G}(P) = 426 μm^2 s^{-1} and D_{R6G}(Mü) = 387 μm^2 s^{-1}. When using the updated values of the diffusion constant, the focal volume and the aggregation number become 84 and 59% higher, respectively.

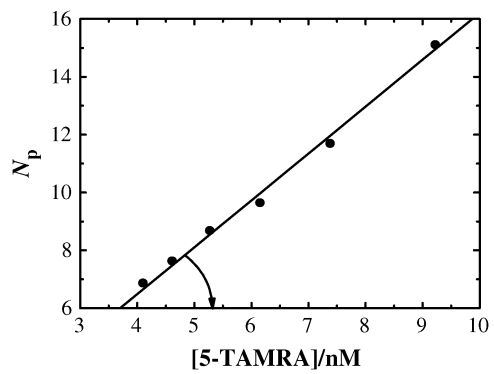

Fig. 7 Calibration of the focal volume by using 5-TAMRA. The slope equals the product $N_A V_f$.

The aggregation numbers of G_{M1} micelles, obtained by using the different calibration methods of FCS are summarised in Table 2. One should note that the calibration using 5-TAMRA provides aggregation numbers with an uncertainty 2–3× less than those obtained by using the diffusion constants. In the determination of the focal volume, the uncertainty is also smaller. The discrepancy between the different approaches to calibration originates in the determination of the structure parameter, together with four other parameters (*cf.* eqn (9)). Irrespective of the calibration method used, the aggregation numbers obtained are spread around the average value of $\bar{N}^{ET}$ = 168. A careful inspection of Table 2 then reveals that N^{FCS}(P) calculated by means of D_{R6G}(P) is closer to $\bar{N}^{ET}$ than N^{FCS}(Mü). Furthermore, N^{FCS}(P) agrees better with N^{FCS}(5-TAMRA). Finally it is worth noting that, when using the old value of the diffusion constant (*i.e.* D_{R6G}(Ma)), the value obtained would be N^{FCS}(Ma) ≈ 91 which agrees poorly with $\bar{N}^{ET}$ = 168.

Aggregation numbers obtained by ET and FCS *versus* LS techniques

While the aggregation numbers determined by FCS and ET are in reasonable agreement, these values differ substantially from those obtained from light scattering experiments. This discrepancy is not surprising because the latter values are mass-averaged aggregation numbers and the micellar size is not strictly monodisperse. An estimate of the polydispersity can be derived by analysing the width at its half-maximum (*cf.* Fig. 1). The corresponding τ_D values are used together with the fact that $D \propto {\tau_D}^{-1}$ and ${R_H}^3 \propto N$. It is then concluded that the particle size may differ by a factor of 3.5. The observant reader might argue that N could depend on the G_{M1} concentration and that the different techniques used here work with quite different concentrations. However, Brocca *et al.*[38] have shown that the micellar size seems to be independent of the concentration in the approximate range of 0.1–100 mM G_{M1}. In addition, the aggregation numbers

Table 2 Aggregation numbers (N^{FCS}) obtained from fluorescence correlation spectroscopy experiments for different calibration methods at 21 °C. The focal volume (V_f) is in units of femtoliters (fl)

	Calibration method				
	Diffusion R6G	Diffusion R6G	Diffusion R6G	5-TAMRA	5-TAMRA
$[G_{M1}]/\mu M$	0.870	0.764	15.4	0.870	0.764
V_f /fl[a]	2.52 ± 0.6	2.49 ± 0.8	2.4 ± 0.9	2.81 ± 0.04	2.78 ± 0.04
V_f /fl[b]	2.18 ± 0.5	2.16 ± 0.65	2.08 ± 0.7	2.81 ± 0.04	2.78 ± 0.04
$N_{p,lim}$	7.94 ± 0.7	6.56 ± 0.6	120 ± 3	7.94 ± 0.7	6.56 ± 0.6
N^{FCS} (Pe)[a]	161 ± 23	169 ± 41	183 ± 61	179 ± 13	189 ± 14
N^{FCS} (Mü)[b]	141 ± 16	148 ± 30	160 ± 49	179 ± 13	189 ± 14

[a] Value D(R6G) = 426 μm^2 s^{-1} at 22.5 °C used to calibrate the focal volume.[24] [b] Value D(R6G) = 414 μm^2 s^{-1} at 25 °C used to calibrate the focal volume.[23]

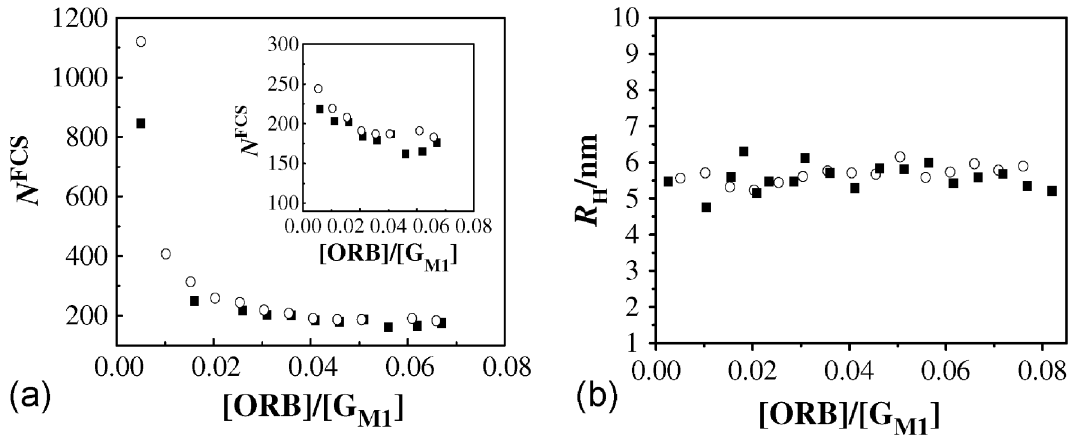

Fig. 8 (a) The convergence behaviour observed for obtaining N^{FCS}. The probe : G_{M1} molar ratio is displayed for $[G_{M1}]$ = 15.4 μM (open circles) and $[G_{M1}]$ = 0.744 μM (black squares). The higher concentration (*ca.* 20×) corresponds to the ET regime. **Insert:** zoomed region for high probe : G_{M1} ratios. (b) The hydrodynamic radius R_H as a function of the probe : G_{M1} molar ratio, obtained for two concentrations of G_{M1} in the bulk: $[G_{M1}]$ = 15.4 μM (open circles) and $[G_{M1}]$ = 0.764 μM (black squares). The higher concentration (*ca.* 20×) corresponds to the ET regime.

obtained by using ET exhibit no significant variation for concentrations ranging from 15.9 to 159 μM (*cf.* Table 1). The values of N^{FCS} (*cf.* Fig. 8) converge to very similar aggregation numbers for the studied concentrations (0.764 and 15.4 μM). The aggregation numbers, as well as the hydrodynamic radius (R_H), remain unaltered when the G_{M1} concentration is increased 20 times (*cf.* Fig. 8B). R_H^{FCS} has been estimated to be 5.67 ± 0.06 nm and this value is in perfect agreement with the LS results (see above). Fig. 8B shows that R_H does not change as the ORB : G_{M1} ratio is varied. This result is not surprising, since the micelles are too small for probing the influence of the extent of labelling as compared to the focal volume.

Conclusions

The light scattering experiments performed on ganglioside G_{M1} micelles are compatible with a rather narrow size distribution, with a mass-averaged aggregation number of 263. This value is significantly larger than the number-averaged aggregation numbers (≈170) calculated from energy transfer and fluorescence correlations spectroscopy data. Taken together, the different techniques show that the micelle size is very similar over a wide range of concentrations (0.764–156 μM).

The results obtained from the ET experiments on G_{M1} micelles have been used to check the calibration of the FCS technique. Although the calibration method gives a reasonably correct value of the aggregation numbers based on knowledge of the correct diffusion constants, a calibration using known dye concentrations (of 5-TAMRA) is preferable. This is because no assumption regarding the shape of the focal volume is needed.

List of abbreviations

A	Acceptor of electronic energy BODIPY-FL-G_{M1}N-(BODIPY-FL-pentanoyl)-ganglioside G_{M1} 564/571-BODIPY-G_{M1}N-(564/570-BODIPY-pentanoyl)-ganglioside G_{M1}
D	Donor of electronic energy
ET	Energy transfer
FCS	Fluorescence correlation spectroscopy
G_{M1}	Ganglioside G_{M1}
LS	Light scattering
M_w^{app}	Apparent molecular mass
N	Aggregation number

N^X	Aggregation number determined by the technique X (ET, FCS or LS)
N_A	Avogadro's constant
N_p	Number of particles in the focal volume
ORB	Octadecylrhodamine B
Pe	Perylene
P_s	Structure parameter
R_H	Hydrodynamic radius
R6G	Rhodamine 6G
5-TAMRA	5-Carboxytetramethylrhodamine
TBPe	Tetra-2,5,8,11-*tert*-Butylperylene
V_f	Focal volume

Acknowledgements

The authors thank Prof. Karel Procházka from the Department of Physical and Macromolecular Chemistry, Charles University, Prague for giving us the opportunity to use the LS equipment. We are grateful to Dr Petr Kadlec from the Institute of Macromolecular Chemistry in Prague for measuring the refractive index increment of G_{M1} molecules. We are also grateful to MSc Erik Rosenbaum for linguistic support. This work was financially supported by the Swedish Research Council (LBÅJ), the Royal Swedish Academy of Science (LBÅJ), the Ministry of Education of the Czech Republic (LC06063, MH) and the Grant Academy of the Czech Republic (GAČR 203/05/H001, RŠ).

References

1 T. Ariga, M. McDonald and R. K. Yu, *J. Lipid Res.*, 2008, **49**, 1157–1175.
2 R. Ledeen and G. Wu, *J. Neurochem.*, 2007, **103**, 126–134.
3 W. Curatolo, *Biochim. Biophys. Acta*, 1987, **906**, 111–136.
4 S. Hakomori, *Curr. Opin. Hematol.*, 2003, **10**, 16–24.
5 C. Dietrich, Z. N. Volovyk, M. Levi, N. L. Thompson and K. Jacobson, *Proc. Natl. Acad. Sci. U. S. A.*, 2001, **98**, 10642–10647.
6 M. Masserini, P. Palestini, B. Venerando, A. Fiorilli, D. Acquotti and G. Tettamanti, *Biochemistry*, 1988, **27**, 7973–7978.
7 C. Yuan, J. Furlong, P. Burgos and L. J. Johnston, *Biophys. J.*, 2002, **82**, 2526–2535.
8 D. Marushchak, N. Gretskaya, I. Mikhalyov and L. B.-Å. Johansson, *Mol. Membr. Biol.*, 2007, **24**, 102–112.
9 K. Yanagisawa, *Neuroscientist*, 2005, **11**, 250–260.
10 N. Brunetti-Pierri and F. Scaglia, *Mol. Genet. Metab.*, 2008, **94**, 391–396.
11 A. T. Aman, S. Fraser, E. A. Merritt, C. Rodigherio, M. Kenny, M. Ahn, W. G. J. Hol, N. A. Williams, W. I. Lencer and T. R. Hirst, *Proc. Natl. Acad. Sci. U. S. A.*, 2001, **98**, 8536–8541.
12 J. Sattler, G. Schwarzmann, I. Knack, K.-H. Rohm and H. Wiegandt, *Hoppe–Seyler's Z. Physiol. Chem.*, 1978, **359**, 719–723.
13 S. Sonnino, L. Cantù, M. Corti, D. Acquotti and B. Venerando, *Chem. Phys. Lipids*, 1994, **71**, 21–45.
14 M. Slevin, S. Kumar, X. He and J. Gaffney, *Int. J. Cancer*, 1999, **82**, 412–423.
15 R. Wang, J. Shi, A. N. Parikh, A. P. Shreve, L. Liaohai Chen and B. I. Swanson, *Colloids Surf. B*, 2004, **33**, 45–51.
16 L. Cantù, M. Corti, E. D. Favero, E. Digirolamo and E. Raudino, *J. Phys. II*, 1996, **6**, 1067–1090.
17 P. Brocca, L. Cantù, M. Cortia, E. D. Favero and A. Raudino, *Physica A*, 2002, **304**, 177–190.
18 D. Orthaber and O. Glatter, *Chem. Phys. Lipids*, 1998, **92**, 53–62.
19 J. Humpolíčková, K. Procházka, M. Hof, Z. Tuzar and M. Špírková, *Langmuir*, 2003, **19**, 4111–4119.
20 T. T. Le, *PNAS*, 2005, **102**, 9160–9164.
21 P. Schwille, U. Haupts, S. Sudipta Maiti and W. W. Webb, *Biophys. J.*, 1999, **77**, 2251–2265.
22 S. Rüttinger, V. Buschmann, B. Krämer, R. Erdmann, R. MacDonald and F. Koberling, in *Confocal, Multiphoton and Nonlinear Microscopic Imaging III*, ed. T. Wilson and A. Periasamy, SPIE-OSA, Munich, 2007, vol. 6630, pp. D66301–D66311.
23 C. B. Müller, A. Loman, V. Pacheco, F. Koberling, D. Willbold, W. Richtering and J. Enderlein, *Europhys. Lett.*, 2008, **83**, 46001.
24 Z. Petrášek and P. Schwille, *Biophys. J.*, 2008, **94**, 1437–1448.
25 D. Magde, E. L. Elson and W. W. Webb, *Biopolymers*, 1974, **13**, 29–61.
26 L. B.-Å. Johansson, G. M. Molotkovsky and L. D. Bergelson, *J. Am. Chem. Soc.*, 1987, **109**, 7374–7381.
27 I. Mikhalyov, N. Gretskaya and L. B.-Å. Johansson, *Chem. Phys. Lipids*, 2009, DOI: 10.1016/j.chemphyslip.2009.01.005.
28 L. Svennerholm, *Methods Carbohydr. Chem.*, 1974, **6**, 464–474.
29 M. Benmouna and W. F. Reed, in *Light Scattering. Principles and Development*, ed. W. Brown, Clarendon Press, Oxford, 1996.
30 J. N. Demas, *Excited state lifetime measurements*, Academic Press, New York, 1983.
31 D. V. O'Connor and D. Phillips, *Time-correlated Single Photon Counting*, Academic Press, London, 1984.
32 B. L. Bales and M. Almgren, *J. Phys. Chem.*, 1995, **99**, 15153–15162.
33 P. P. Infelta, M. Grätzel and J. K. Thomas, *J. Phys. Chem.*, 1974, **78**, 190.
34 M. Tachiya, *Chem. Phys. Lett.*, 1975, **33**, 289–292.
35 A. Benda, M. Hof, M. Wahl, M. Patting, R. Erdmann and P. Kapusta, *Rev. Sci. Instrum.*, 2005, **76**, Art. No. 033106.
36 D. Magde, E. L. Elson and W. W. Webb, *Phys. Rev. Lett.*, 1972, **29**, 705.
37 W. W. Webb, in *Fluorescence Correlation Spectroscopy Theory and Applications*, ed. R. Rigler, E. S. Elson, Springer-Verlag, Berlin, 2001.
38 P. Brocca, M. Corti, E. D. Favero and E. A. Raudino, *Langmuir*, 2007, **23**, 3067–3074.
39 F. Bergström, I. Mikhalyov, P. Hägglöf, R. Wortmann, T. Ny and L. B.-Å. Johansson, *J. Am. Chem. Soc.*, 2002, **124**, 196–204.
40 B. Ulrich-Bott and H. Wiegandt, *J. Lipid Res.*, 1984, **25**, 1233.
41 S. Yokoyama, T. Takeda and M. Abe, *Biointerfaces*, 2001, **20**, 361.